KI REPORTS
KIReports.org
TRANSLATIONAL RESEARCH

# Single-Nucleus RNA-Sequencing Identifies a Differential Profibrotic Response in Parietal Epithelial Cells in Primary Versus Maladaptive Focal Segmental Glomerulosclerosis

Dries Deleersnijder[1], Tom Venken[2], Rogier Schepers[2], Thomas Van Brussel[2], Björn K. Meijers[1,3], Ben Sprangers[4,5], Diether Lambrechts[2] and Amaryllis H. Van Craenenbroeck[1,3]

[1]Department of Microbiology, Nephrology and Renal Transplantation Research Group, Immunology and Transplantation, KU Leuven, Leuven, Belgium; [2]Department of Human Genetics, Laboratory of Translational Genetics, VIB-KU Leuven, Leuven, Belgium; [3]Division of Nephrology, University Hospitals Leuven, Leuven, Belgium; [4]Department of Nephrology, Ziekenhuis Oost-Limburg, Genk, Belgium; and [5]Department of Immunology and Infection, Biomedical Research Institute, UHasselt, Diepenbeek, Belgium

**Introduction:** Focal segmental glomerulosclerosis (FSGS) lesions occur in a wide range of clinical conditions that are all characterized by critical podocyte injury. Differentiating primary from maladaptive forms of FSGS remains challenging because of the absence of reliable biomarkers, resulting from a lack of insight into their pathophysiological differences.

**Methods:** We used single-nucleus RNA-sequencing (snRNA-seq) to identify differentially expressed transcriptional signatures in kidney biopsies of well-phenotyped primary versus maladaptive FSGS. We included cryopreserved kidney biopsy cores from adult patients with newly diagnosed primary FSGS ($n = 9$, all nephrotic), maladaptive FSGS ($n = 9$, all nonnephrotic), proteinuric controls (antiphospholipase A2 receptor antibody–positive membranous nephropathy [PLA2R+ MN], $n = 3$), and healthy controls ($n = 4$).

**Results:** We identified 120,751 high-quality nuclei, including 2471 podocytes and 1574 parietal epithelial cells (PECs). In primary FSGS, podocytes showed a more pronounced but not specific injury pattern with upregulation of immune pathways, such as antigen presentation, and mammalian target of rapamycin (mTOR) complex 1 (mTORC1)-signaling. Glomerular cell-cell interaction analysis showed increased profibrotic TGF-β and PDGFR-β signaling in primary FSGS PECs, which also upregulated genes that compose the normal PEC-derived extracellular matrix (ECM) (*LAMB1, COL4A1, COL4A5, COL4A6*). In maladaptive FSGS, podocytes showed few differentially expressed genes (DEGs) and PEC-PEC interactions predominated. Here, a (myo-)fibroblast-like PEC subpopulation upregulated non–type IV fibril- and network-forming collagens (*COL1A1, COL5A1, COL8A1*), which may further contribute to the development of glomerulosclerosis.

**Conclusion:** This study presents a single-cell transcriptional landscape of well-phenotyped patients with FSGS and provides evidence for a differential profibrotic PEC response in primary versus maladaptive FSGS.

*Kidney Int Rep* (2025) **10,** 3255–3270; https://doi.org/10.1016/j.ekir.2025.06.023
KEYWORDS: fibrosis; focal segmental glomerulosclerosis; FSGS; single-nucleus RNA-sequencing; snRNA-seq; transcriptomics


FSGS is defined by the microscopic appearance of scar tissue ("sclerosis") in segments of some ("focal") glomeruli.[1,2] FSGS lesions occur in a wide range of clinical conditions, also referred to as podocytopathies, which are characterized by severe podocyte injury and loss.[2,3] FSGS is currently subdivided into primary, secondary and genetic forms.[1] Primary FSGS is an autoimmune disease that is attributed to

**Correspondence:** Amaryllis H. Van Craenenbroeck, Nephrology and Renal Transplantation Research Group, KU Leuven, Department of Microbiology, Immunology and Transplantation, KU Leuven, UZ Herestraat 49, 3000 Leuven, Belgium. E-mail: amaryllis.vancraenenbroeck@kuleuven.be

**Received 1 May 2025; accepted 9 June 2025; published online 18 June 2025**

unknown circulating permeability factors that cause generalized podocyte injury.[1,2] Secondary FSGS most often arises because of glomerular hypertension, in which there is a mismatch between glomerular load and capacity, and is therefore referred to as maladaptive FSGS.[4] The genetic forms of FSGS result from pathogenic variants in genes that encode for podocyte proteins or collagen type IV.[1,2,5] Primary FSGS is treated with immunosuppressive therapy, whereas this is contraindicated in maladaptive and genetic FSGS.[6]

Despite the heterogeneous underlying etiologies of FSGS, its initial clinical and histopathologic presentation may be very similar. Currently, the Kidney Disease: Improving Global Outcomes (KDIGO) guidelines recommend differentiating the underlying FSGS etiology based on the presence of nephrotic syndrome, exclusion of secondary causes, and the extent of podocyte foot process effacement on electron microscopy.[6] There are no other reliable serum, urine, or histopathologic biomarkers available that can differentiate between FSGS etiologies, making the diagnosis challenging.[2] Furthermore, in previous studies, patient stratification according to the presumed underlying etiology was often not performed or flawed, potentially invalidating the reported results.[2] Clearly, our current pathophysiological understanding of the different etiologies of FSGS is insufficient.

At the mechanistic level, podocytes in FSGS become critically injured and detach from the glomerular basement membrane. This leaves regions of the glomerular basement membrane uncovered, resulting in proteinuria.[2] In response, the adjacent PECs become activated, proliferate, and migrate toward the glomerular capillary tuft, where they deposit ECM against the glomerular basement membrane.[7-10] This results in the typical sclerotic FSGS lesion seen on kidney biopsy.

Given the different etiologies that underly FSGS lesions, we hypothesized that gene expression profiles within glomerular cells could differ between FSGS subtypes. Previous transcriptomics studies in FSGS insufficiently stratified according to the underlying etiology and did not provide single-cell resolution, which might be necessary to study less abundant glomerular cells in this focal disease.[11] In this study, we used snRNA-seq to identify single-cell gene expression signatures in kidney biopsies of well-phenotyped primary versus maladaptive patients with FSGS to gain more insights into their underlying pathophysiology.

## METHODS

### Ethics

This study was approved by the Ethical Committee of the University Hospitals Leuven (study references S53364, S54095 and S65227). All study participants provided written informed consent.

### Study Design and Included Patients

We included adult patients who underwent core needle native kidney biopsy at the University Hospitals of Leuven, Belgium, between 2017 and 2022. Cryopreserved kidney tissue was available from the Leuven Renal Research Biobank (S54095) and Biobank Kidney Transplantation (S53364). Only 1 biopsy per patient was used. We used a total of 25 samples, including 9 primary FSGS samples, 9 maladaptive FSGS samples, 3 control samples with proteinuria (all PLA2R+ MN) and 4 healthy control samples.

### Clinicopathologic Characterization of Included Patients

The inclusion criteria of patients with newly diagnosed primary FSGS, maladaptive FSGS, and PLA2R+ MN are shown in Table 1, in accordance with the Kidney Disease: Improving Global Outcomes (KDIGO) guidelines.[6] Healthy control samples were obtained from healthy individuals undergoing living kidney donation. These were preperfusion biopsies with short ischemia times, in which histopathology showed no abnormalities. Individual characteristics of included patients and controls are outlined in Supplementary Tables S1 to S3. In 1 patient with maladaptive phenotype, genetic analysis revealed a likely pathogenic splice mutation in the *COL4A3* gene. In all other patients, genetic analysis was either negative or not performed.

### Definition of Outcome Parameters

Complete remission was defined as follows: (i) reduction of urine protein-to-creatinine ratio $< 0.3$ g/g, and (ii) stable kidney function ($< 15\%$ estimated glomerular filtration rate decline compared with baseline), and (iii) serum albumin $> 35$ g/l, for at least 3 months.[6] Kidney failure was defined as the start of kidney replacement therapy.

### Sample Collection

In patients with a diagnosis of FSGS or PLA2R+ MN, percutaneous ultrasound-guided biopsies were performed with a 16G needle, and half of 1 biopsy core was used for research. In healthy individuals undergoing living kidney donation, a perioperative preperfusion biopsy was obtained with a 16G needle and the entire biopsy was used for research. All biopsies were immediately submerged in AllProtect Tissue Reagent (Qiagen) for stabilization of the transcriptome and subsequently cryopreserved at $-20$ °C.

**Table 1.** Patient inclusion criteria

| | Primary FSGS | Maladaptive FSGS | PLA2R+ MN |
|---|---|---|---|
| Presence of nephrotic syndrome at biopsy[a] | Yes, present | No, absent | May either be present or absent |
| Proteinuria at biopsy[b] | ≥ 3.5 g/g or ≥ 3.5 g per 24 h | < 3.5 g/g and < 3.5 g per 24 h | ≥ 1.0 g/g or ≥ 1.0 g per 24 h |
| Secondary causes of FSGS | Excluded | Present, related to glomerular hypertension | NA |
| Light microscopy | At least one FSGS lesion, absence of other primary glomerular disease | At least one FSGS lesion, absence of other primary glomerular disease | Injury pattern of membranous nephropathy, no FSGS lesions |
| Immunofluorescence/Immunohistochemistry | Negative (trace of IgM and/or C3/C3d was allowed) | Negative (trace of IgM and/or C3/C3d was allowed) | Glomerular positivity for IgG and C3/C3d, positive for PLA2R1 |
| Electron microscopy | ≥ 80% podocyte FPE[c] | < 80% podocyte FPE[d] | Any FPE |
| Immunosuppressive (IS) treatment | No active IS treatment at kidney biopsy. After biopsy, all patients were treated with IS treatment | No active IS treatment at kidney biopsy. No patients were treated with IS after biopsy. | No active IS treatment at kidney biopsy. |
| Serum antibodies | NA | NA | Positive anti-PLA2R antibodies (> 20 RU/ml, measured by ELISA) |

Anti-PLA2R antibodies, antiphospholipase A2-receptor antibodies; ELISA, enzyme-linked immunoassay; FPE, foot process effacement; FSGS, focal segmental glomerulosclerosis; MN, membranous nephropathy; NA, not applicable; PLA2R+ MN, antiphospholipase A2 receptor antibody–positive membranous nephropathy; UPCR, urine protein-to-creatinine ratio.
[a]Nephrotic syndrome was defined by serum albumin < 35 g/l, urine protein-to-creatinine ratio (UPCR) ≥ 3.5 g/g or proteinuria ≥3.5 g on 24 h urinary collection and presence of edema.
[b]Either UPCR or proteinuria on 24 h urinary collection.
[c]Electron microscopy study was available in 7 out of 9 primary FSGS samples.
[d]Electron microscopy study was available in 7 out of 9 maladaptive FSGS samples.

## Sample Processing and snRNA-seq Protocol

Details are provided in the Supplementary Methods. In brief, nuclei were isolated on ice,[12] and snRNA-seq libraries were prepared using the Chromium Single Cell 3′ reagent kit v3.1 (10x Genomics, Pleasanton, CA). Libraries were sequenced on the NovaSeq 6000 (Illumina, San Diego, CA).

## snRNA-seq Data Analysis

Details are provided in the Supplementary Methods. In brief, reads were aligned to the genome using Cell Ranger (10x Genomics) (Supplementary Data S1). Next, samples were corrected for ambient RNA contamination using CellBender.[13] Nuclei with > 1000 and < 4000 genes per nucleus and < 5% mitochondrial RNA were retained. Doublets were detected using DoubletFinder.[14] Next steps included data normalization, scaling, principal component analysis, sample integration using Harmony,[15] and cell annotation. We identified 120,751 high-quality nuclei for downstream analysis (Figure 1). Quality control metrics of the final dataset are shown in Supplementary Figures S1 to S3 and Supplementary Data S2. Differential gene expression analysis between cell clusters was done using the *FindAllMarkers*-function (Wilcoxon rank sum test). DEGs of annotated clusters are shown in Supplementary Data S3. Differential gene expression analysis between diagnostic groups was done with a pseudobulk method from the EdgeR-package,[16] because pseudobulk methods preserve intersample variability and decrease false discovery rate.[17] False discovery rate-values < 0.10 were considered significant. Gene set enrichment analysis (GSEA) was done with the fgsea package (Benjamini-Hochberg adjusted *P*-value < 0.05 considered significant).[18] Differential glomerular cell-cell communication across diagnostic groups was done with MultiNicheNet.[19] MultiNicheNet addresses intersample heterogeneity, thereby reducing false discoveries.[19]

## Statistical Analysis

Baseline characteristics and cell type abundances were described by median and interquartile range for continuous variables (nonnormally distributed), and by frequencies and percentages for categorical variables. Differences in cell type abundance between > 2 groups were assessed with Kruskal–Wallis tests and Bonferroni-corrected Dunn tests for *post hoc* pairwise comparisons. Adjusted *P*-values < 0.05 were considered significant.

# RESULTS

## Clinicopathologic Characterization of Patients With FSGS and Controls

We processed kidney biopsies from patients with newly diagnosed primary FSGS ($n = 9$) and maladaptive FSGS ($n = 9$) by snRNA-seq (Figure 1a). All patients with primary FSGS were nephrotic, showed ≥ 80% foot process effacement on kidney biopsy (electron microscopy available in 7/9 biopsies) and were treated with corticosteroid monotherapy after kidney biopsy (Table 2). None of the patients with maladaptive FSGS were nephrotic; all showed < 80% foot process effacement (electron microscopy available in 7/9 biopsies) and none were treated with immunosuppressive agents. We included control samples from patients with newly diagnosed PLA2R+ MN ($n = 3$, controls with proteinuria) and healthy individuals undergoing living kidney donation ($n = 4$). Baseline patient characteristics are shown in Table 2 (details in Supplementary Tables S1 to S3). The degree of disease chronicity on kidney biopsy, summarized by the Mayo

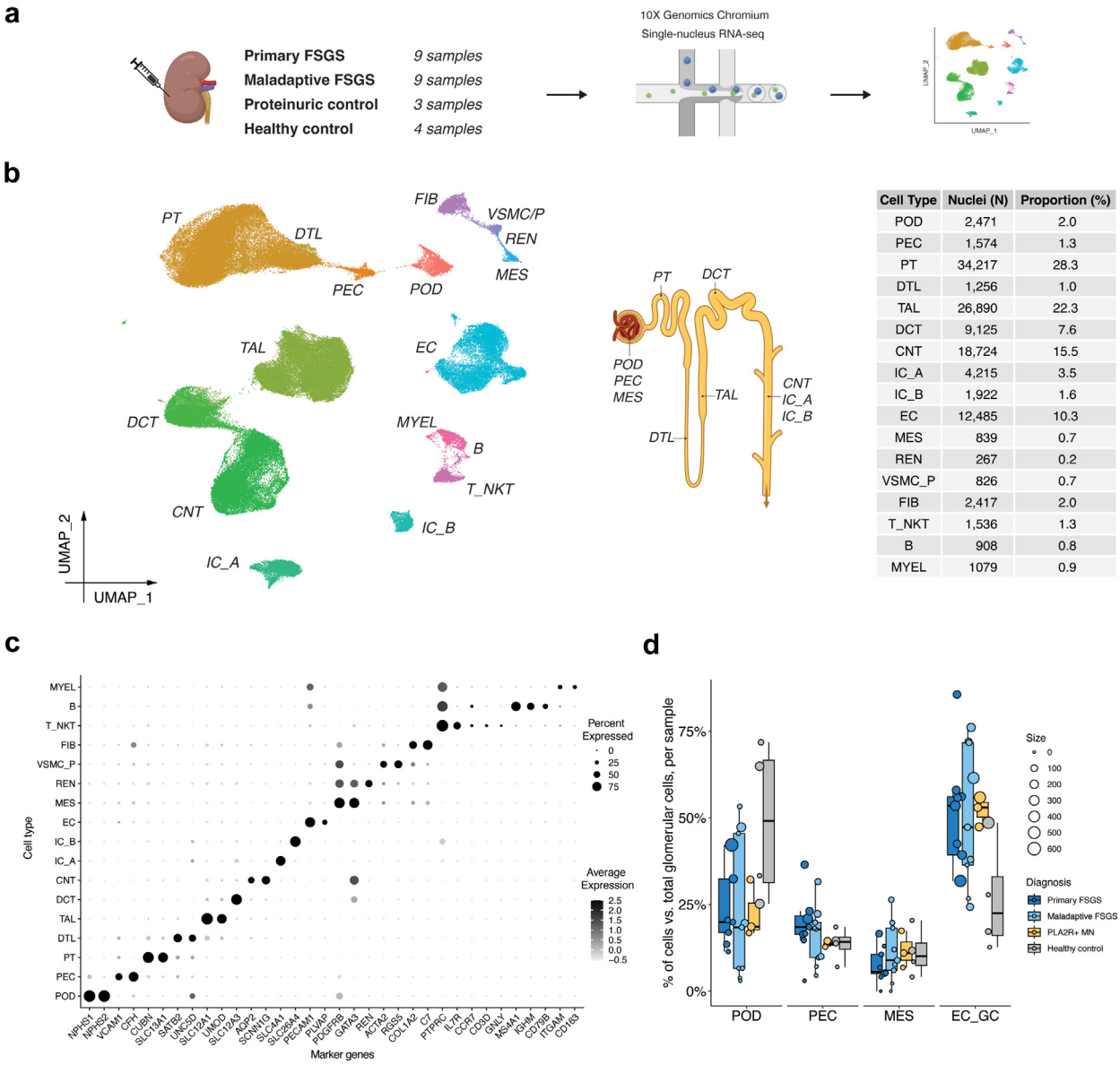


**Figure 1.** Identification of kidney cell subtypes and glomerular cell abundance analysis. (a) Experimental design. (b) UMAP plot and table of all identified kidney cells after QC ($n$ = 120,751 nuclei) and schematic of the normal human nephron. (c) Dot plot showing expression of marker genes per cluster. The size of the dot reflects the fraction of cells (%) in which the gene is expressed, the intensity of the dot reflects average expression level. (d) Glomerular cell type abundance analysis. Box plots reflect median and IQR. The size of dots reflects the absolute number of cells in the sample. Differences between diagnostic groups were tested with Kruskal-Wallis test and all were not significant. B, B cell; CNT, connecting tubule cell; DCT, distal convoluted tubule cell; DTL, loop of Henle, descending thin limb, EC, endothelial cell; EC_GC, glomerular capillary endothelial cell; FIB, fibroblast; IC_A/B, type A/B intercalated cell; IQR, interquartile range; MES, mesangial cell; MYEL, myeloid cell; PEC, parietal epithelial cell; POD, podocyte; PT, proximal tubule cell; QC, quality control; REN, renin-producing cell; TAL, loop of Henle, thick ascending limb cell; T_NKT, T cell and NK cell; VSMC_P, vascular smooth muscle cell/pericyte. Parts of panels (a) and (b) were made with BioRender.

Clinic Chronicity Score,[20] was higher in maladaptive FSGS (6.0, interquartile range: 4.0-7.0) versus primary FSGS (2.0, interquartile range: 1.0–4.0) and PLA2R+ MN (1, interquartile range: 1.0–1.5).

## Kidney Cell Annotation and Differential Abundance Testing Across Diagnostic Groups

We identified a total of 120,751 high-quality nuclei, which, based on marker gene expression, could be assigned to all major kidney cell types (Figures 1b and c). To correct for the varying number of glomeruli present in each biopsy sample, we calculated glomerular cell abundances across the 4 diagnostic groups relative to the total number of glomerular cells in the biopsy, rather than the total number of all kidney cells (Figure 1d). No significant differences between groups were observed. Podocyte abundances varied substantially between samples; however, FSGS samples did not

**Table 2.** Baseline characteristics

| Characteristics | Primary FSGS ($n$ = 9) Median (IQR) or $n$ (%) | | Maladaptive FSGS ($n$ = 9) Median (IQR) or $n$ (%) | | PLA2R+ MN ($n$ = 3) Median (IQR) or $n$ (%) | | Healthy ($n$ = 4) Median (IQR) or $n$ (%) | |
|---|---|---|---|---|---|---|---|---|
| Demographics and comorbidities | | | | | | | | |
| Age at biopsy, yrs | 46.1 | (38.7–66.5) | 51.3 | (37.8–63.5) | 65.2 | (63.0–67.2) | 46.5 | (36.5–57.8) |
| Sex, male | 6 | (66.7) | 8 | (88.9) | 2 | (66.7) | 1 | (25.0) |
| Ethnicity, White | 9 | (100.0) | 9 | (100.0) | 3 | (100.0) | 4 | (100.0) |
| BMI, at biopsy (kg/m$^2$) | 27.7 | (24.6–29.4) | 29.4 | (23.5–33.4) | 25.9 | (25.2–28.5) | 23.3 | (22.0–24.8) |
| OSAS, at biopsy | 2 | (22.2) | 3 | (33.3) | 0 | (0.0) | | |
| Hypertension, at biopsy | 5 | (55.6) | 7 | (77.8) | 3 | (100.0) | 0 | (0.0) |
| Current/former smoker, at biopsy | 4 | (44.4) | 5 | (55.6) | 2 | (66.7) | 0 | (0.0) |
| Diabetes mellitus, at biopsy | 2 | (22.2) | 4 | (44.4) | 0 | (0.0) | 0 | (0.0) |
| Clinical and biochemical characteristics | | | | | | | | |
| RAAS inhibitor use, at biopsy | 5 | (55.6) | 6 | (66.7) | 2 | (66.7) | 0 | (0.0) |
| Immunosuppressant use, at biopsy | 0.0 | (0.0) | 0.0 | (0.0) | 0.0 | (0.0) | 0 | (0.0) |
| Edema, at biopsy | 9 | (100.0) | 1 | (11.1) | 3 | (100.0) | 0 | (0.0) |
| Hematuria, at biopsy | 7 | (77.8) | 3 | (33.3) | 3 | (100.0) | 2[a] | (50.0) |
| UPCR, highest[b] | 8.6 | (7.9–10.9) | 2.1 | (0.3–3.0) | 5.5 | (4.5–6.9) | 0.0 | (0.0–0.0) |
| UPCR, at biopsy | 4.9 | (3.7–7.8) | 1.7 | (0.2–1.9) | 5.0 | (3.2–5.4) | 0.0 | (0.0–0.0) |
| sAlb, at biopsy (g/l) | 22.6 | (19.4–27.0) | 41.3 | (41.2–42.9) | 28.2 | (25.4–30.4) | 47.6 | (46.2–48.0) |
| sCr, at biopsy (mg/dl) | 1.1 | (1.0–1.4) | 1.7 | (1.1–2.5) | 1.1 | (0.9–1.1) | 0.8 | (0.8–0.8) |
| eGFR, at biopsy (ml/min per 1.73 m$^2$) | 69.0 | (60.0–108.0) | 42.0 | (32.0–65.0) | 70.0 | (69.0–80.0) | 92.0 | (91.5–98.3) |
| Genetics performed | 4 | (44.4) | 5 | (55.6) | 0 | (0.0) | 0 | (0.0) |
| Histopathologic features | | | | | | | | |
| Percentage of glomeruli with FSGS lesions on LM | 9.5 | (6.5–18.2) | 12.5 | (9.1–20.0) | 0.0 | (0.0–0.0) | 0.0 | (0.0–0.0) |
| Percentage of glomeruli with global sclerosis on LM | 0.0 | (0.0–5.6) | 36.4 | (18.2–40.0) | 5.6 | (4.6–6.0) | 0.0 | (0.0–1.3) |
| GS | 0.0 | (0.0–1.0) | 2.0 | (2.0–2.0) | 0.0 | (0.0–0.0) | 0.0 | (0.0–0.0) |
| IF | 1.0 | (0.0–1.0) | 2.0 | (1.0–2.0) | 0.0 | (0.0–1.0) | 0.0 | (0.0–0.0) |
| TA | 1.0 | (0.0–1.0) | 2.0 | (1.0–2.0) | 0.0 | (0.0–0.0) | 0.0 | (0.0–0.0) |
| CV | 0.0 | (0.0–1.0) | 0.0 | (0.0–1.0) | 1.0 | (0.5–1.0) | 0.0 | (0.0–0.0) |
| MCCS | 2.0 | (1.0–4.0) | 6.0 | (4.0–7.0) | 1.0 | (1.0–1.5) | 0.0 | (0.0–0.0) |
| EM performed | 7 | (77.8) | 7 | (77.8) | | | | |
| FPE ≥ 80% | 7 | (100.0)[c] | 0 | (0.0)[c] | | | | |
| Initiated treatment(s) and outcomes | | | | | | | | |
| CS monotherapy | 9 | (100.0) | 0 | (0.0) | 0 | (0.0) | | |
| CS + CNI | 3 | (33.3) | 0 | (0.0) | 0 | (0.0) | | |
| Follow-up time, mo[d] | 27.2 | (13.7–46.7) | 32.3 | (24.6–35.1) | 51.6 | (37.2–53.2) | | |
| First complete remission | 7 | (77.8) | 3 | (33.3) | 1 | (33.3) | | |
| Kidney failure | 1 | (11.1) | 2 | (22.2) | 0 | (0.0) | | |
| Death | 1 | (11.1) | 0 | (0.0) | 0 | (0.0) | | |

BMI, body mass index; CS, corticosteroid; CNI, calcineurin inhibitor; CV, arteriosclerosis (score 0–1, part of total MCCS); eGFR, estimated glomerular filtration rate; EM, electron microscopy; FPE, foot process effacement; FSGS, focal segmental glomerulosclerosis; GS, glomerulosclerosis (score 0–3, part of total MCCS); IF, interstitial fibrosis (score 0–3, part of total MCCS); IQR, interquartile range; LM, light microscopy; MCCS, Mayo Clinic Chronicity Score; MN, membranous nephropathy; OSAS, obstructive sleep apnea syndrome; PLA2R+ MN, antiphospholipase A2 receptor antibody–positive membranous nephropathy; RAAS, renin-angiotensin-aldosterone system; sAlb. serum albumin; sCr, serum creatinine; TA, tubular atrophy (score 0–3, part of total MCCS); UPCR, urine protein-to-creatinine ratio.
[a]Hematuria in healthy donors was only sporadic and not continuous.
[b]Highest proteinuria in the time interval of 3 months up until biopsy.
[c]Percentage calculated in patients where EM was performed.
[d]Time period between kidney biopsy date and last nephrological consultation in months.

exhibit overt podocytopenia. Cell type abundance analysis of all cells in the total kidney cell population is shown in Supplementary Figures S4 and S5.

## Primary FSGS Podocytes Upregulate Immune Pathways and MTORC1 Signaling

We identified 2471 high-quality podocytes (*NPHS1*+, *NPHS2*+) (Supplementary Figures S6 and S7, Supplementary Data S4). We performed differential gene expression analysis between podocytes from 1 diagnostic group relative to those from the other 3 groups, revealing the top DEGs per diagnosis (Figure 2a, Supplementary Data S5). Significantly upregulated DEGs in primary FSGS podocytes included ECM protein 1 (*ECM1*), semaphorin 4G (*SEMA4G*), EH domain containing 4 (*EHD4*), zinc finger protein 44 (*ZNF44*) and 250 (*ZNF250*), and pleckstrin homology like domain family B member 1 (*PHLDB1*) (Figure 2a

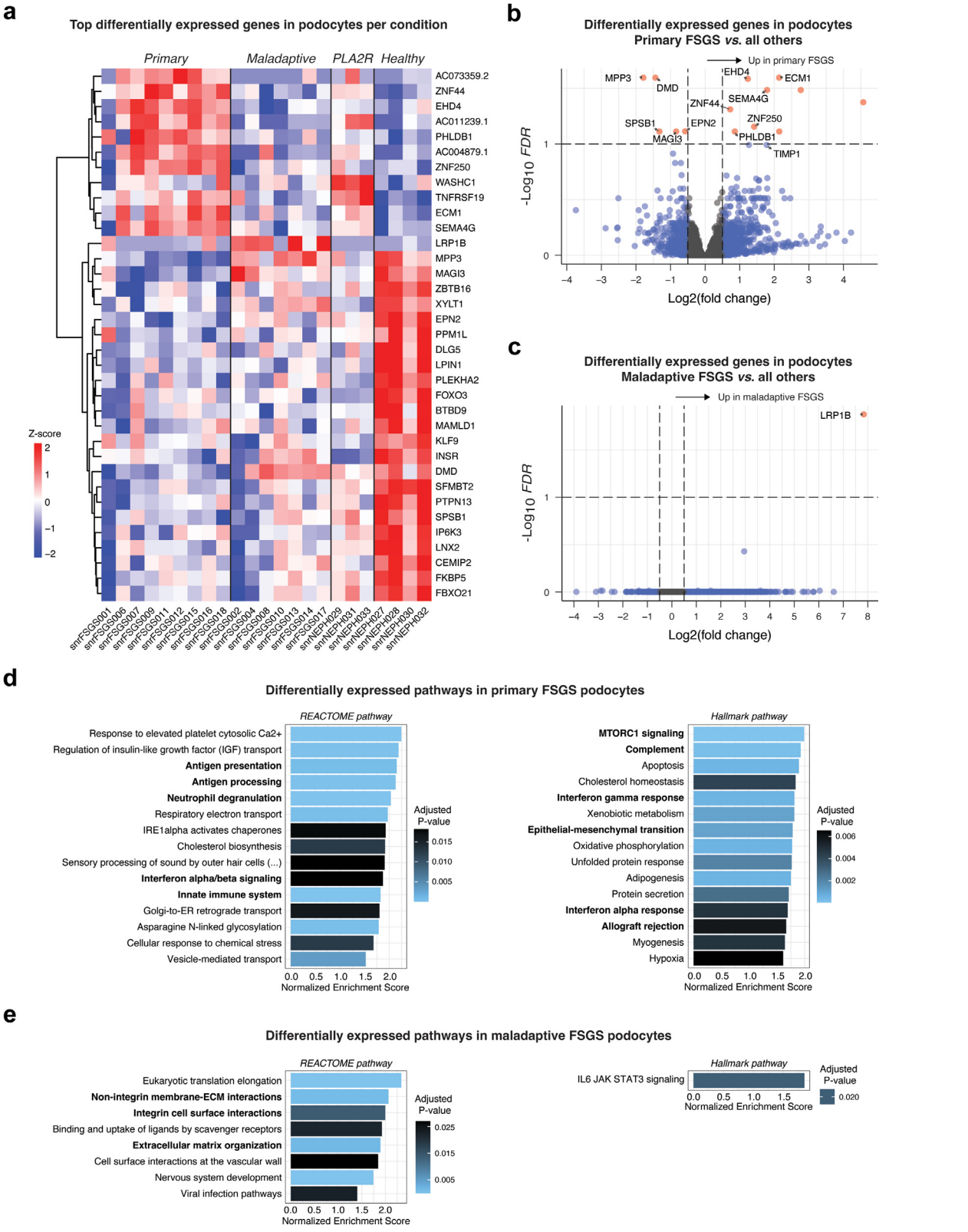


**Figure 2.** Differential gene expression analysis in all podocytes. (a) Heatmap showing the top 20 most significant DEGs in podocytes per diagnostic group (EdgeR pseudobulk expression, absolute $\log_2FC > 0.50$ or $\log_2FC < -0.50$, adjusted *P*-value (FDR) $< 0.10$), allowing hierarchical clustering of genes (rows). Two maladaptive FSGS samples were not retained in the DEG analysis due to small pseudobulk library sizes (< 50,000 counts). Z-scores were calculated per row. Only the healthy subgroup showed > 20 significant DEGs. (b) Volcano plot depicting DEGs in primary FSGS podocytes versus all other podocytes (red dots: absolute $\log_2FC > 0.50$ or $\log_2FC < -0.50$, adjusted *P*-value (FDR) $< 0.10$). (c) Volcano plot depicting DEGs in maladaptive FSGS podocytes versus all other podocytes (red dots: absolute $\log_2FC > 0.50$ or $\log_2FC < -0.50$, adjusted *P*-value (FDR) $< 0.10$). (d) Top 15 most significant pathways identified using GSEA on DEGs in primary FGSG podocytes versus other podocytes, using Reactome (left panel) and Hallmark (right panel) gene sets. (e) All significant pathways identified using GSEA on (continued)

and b). Subsequent GSEA in primary FSGS podocytes showed upregulation of immune pathways involved in antigen presentation and processing, driven by upregulation of major histocompatibility complex class I protein coding genes (*HLA-A, HLA-B, HLA-C, HLA-E, B2M*), proteasome 20S subunit alpha 3 (*PSMA3*) and calreticulin (*CALR*) (Figure 2d, Supplementary Data S6). Other immune pathways involved complement genes (*C1R, C1S*) and interferon response (*ADAR, IFI6*). Primary FSGS podocytes also showed upregulation of the MTORC1 signaling pathway (normalized enrichment score [NES] 2.0, $P < 0.001$) (Figure 2d). Differential gene expression testing between primary FSGS podocytes and control podocytes yielded similar results (Supplementary Figure S8). In contrast, testing between primary and maladaptive FSGS podocytes showed only 1 DEG (*DMD*) and no pathways (Supplementary Figure S9), suggesting transcriptional similarity between these 2 FSGS subtypes. When plotting podocyte expression of genes enriched in the immune and mTORC1-signaling pathways, some maladaptive FSGS samples indeed also showed mild upregulation (Supplementary Figure S10 and S11). Considering the recent discovery of pathogenic anti-nephrin autoantibodies in podocytopathies,[21,22] we also compared gene expression of nephrin (*NPHS1*) across the 4 diagnostic groups, which showed no clear differences (Supplementary Figure S12). Altogether, our analyses suggest some transcriptional similarity in primary and maladaptive FSGS podocytes, indicating that the observed signatures are likely not specific for primary FSGS, but may be more pronounced.

## Maladaptive FSGS Podocytes Are Heterogeneous and Show Few DEGs

When comparing maladaptive FSGS podocytes to all other diagnostic groups, LDL receptor–related protein 1B (*LRP1B*) was the only significantly upregulated gene (Figure 2c). GSEA additionally identified upregulation of the ECM organization pathway (NES 1.9, $P = 0.002$), which remained upregulated when comparing maladaptive FSGS podocytes with only control podocytes (NES 2.1, $P < 0.001$) (Figure 2e, Supplementary Figures S13 and S14). This pathway also appeared upregulated in primary FSGS podocytes (NES 1.7, $P = 0.019$) (Supplementary Figure S8), again confirming the transcriptional overlap between podocytes from both FSGS subgroups.

## Primary FSGS PECs Show Profibrotic PDGFR-β and TGF-β Signaling and Upregulate PEC Basement Membrane Genes

Next, we identified 1574 high-quality PECs (*VCAM1+, CFH+*) (Supplementary Figures S15 and S16, Supplementary Data S7). Similar to our analysis within podocytes, we first performed differential gene expression analysis between PECs from 1 diagnostic group relative to those from the other 3 groups (Figure 3a, Supplementary Data S8). Primary FSGS PECs exhibited upregulation of platelet-derived growth factor receptor beta (*PDGFRB*), signal transducer and activator of transcription 1 (*STAT1*) and the ECM regulator cathepsin C (*CTSC*) (Figure 3b). GSEA indicated profibrotic signaling with upregulation of ECM organization (NES 1.7, $P = 0.007$) and PDGF signaling (NES 1.9, $P = 0.008$) (Figure 3d, Supplementary Data S9). When comparing primary FSGS PECs to only control PECs, the ECM organization pathway remained upregulated (Supplementary Figure S17). When comparing solely primary to maladaptive FSGS PECs, genes related to degradation of ECM appeared upregulated (Supplementary Figure S18). To further elucidate this ECM signature, we plotted the individual genes enriched in the ECM organization pathway (Figure 4). Primary FSGS PECs upregulated ADAMTS enzymes (*ADAMTS1*, *ADAMTS2*, *ADAMTS5*), which may be involved in tissue remodeling.[23] Thrombospondin 1 (*THBS1*) and integrin subunit beta 8 (*ITGB8*) were also upregulated, which both play a key role in activation of latent TGF-β-1 and thus, the activation of the profibrotic TGF-β pathway. Primary FSGS PECs also upregulated genes composing the normal PEC basement membrane[24]; including laminin subunit beta 1 (*LAMB1*); collagen type IV alpha 1 chain (*COL4A1*, involved in the collagen IVα121 trimer); and collagen type IV alpha 5 (*COL4A5)* and 6 chains (*COL4A6*, both involved in the collagen IVα556 trimer) (Figure 4). Taken together, primary FSGS PECs clearly demonstrated a profibrotic response with upregulation of PDGFR-β and TGF-β signaling, and type IV collagen genes.

## A Subpopulation of Maladaptive FSGS PECs Adopt a (Myo-)fibroblast-Like Phenotype

When comparing maladaptive FSGS PECs to all other diagnostic groups, integrin subunit alpha 11 (*ITGA11*) was amongst the top upregulated genes (Figure 3c). When comparing only maladaptive with primary FSGS

**Figure 2.** (continued) DEGs in maladaptive FGSG podocytes versus other podocytes, using Reactome (left panel) and Hallmark (right panel) gene sets. Pathways in bold are discussed further in the main text. DEG, differentially expressed genes; FDR, false discovery rate; FSGS, focal segmental glomerulosclerosis; GSEA, gene set enrichment analysis.

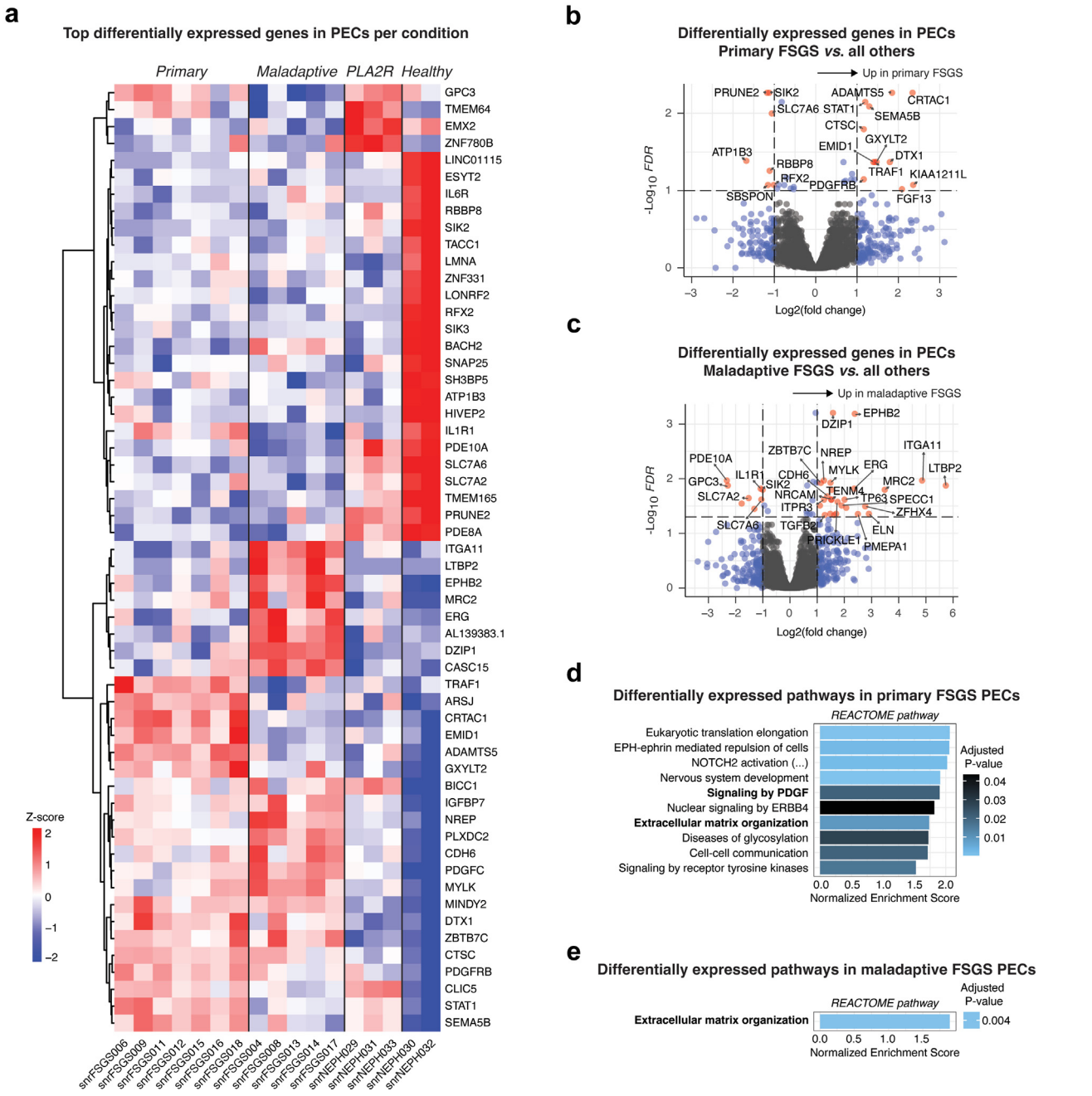


**Figure 3.** Differential gene expression analysis in all PECs. (a) Heatmap showing the top 20 most significant DEGs in PECs per diagnostic group (EdgeR pseudobulk expression, absolute $\log_2$FC $>$ 0.50 or $\log_2$FC $<$ −0.50, adjusted *P*-value (FDR) $<$ 0.10), allowing hierarchical clustering of genes (rows). Eight samples were not retained in the DEG analysis due to small pseudobulk library sizes ($<$ 50,000 counts). (b) Volcano plot depicting DEGs in primary FSGS PECs versus all other PECs (red dots: absolute $\log_2$FC $>$ 1.00 or $\log_2$FC $<$ −1.00, adjusted *P*-value (FDR) $<$ 0.10). (c) Volcano plot depicting DEGs in maladaptive FSGS PECs versus all other PECs (red dots: absolute $\log_2$FC $>$ 1.00 or $\log_2$FC $<$ −1.00, adjusted *P*-value (FDR) $<$ 0.05). (d) Significant pathways identified using GSEA on DEGs in primary FGSG PECs versus other PECs. (e) Maladaptive FSGS PECs versus other PECs, using Reactome gene sets. Pathways in bold are discussed further in the main text. DEG, differentially expressed gene; FSGS, focal segmental glomerulosclerosis; GSEA, gene set enrichment analysis; PEC, parietal epithelial cell.

PECs, *ITGA11* remained the most prominent upregulated "matrisome"-associated gene (Figure 4c). Similar to primary FSGS, GSEA in maladaptive FSGS PECs showed upregulation of the ECM organization pathway (NES 1.9, $P = 0.002$) (Figure 3e). When comparing maladaptive FSGS PECs to only control PECs, no differentially expressed pathways reached statistical significance, although the ECM organization pathway remained upregulated (NES 1.7, $P = 0.18$). When plotting the genes upregulated in this pathway (Figure 4a and b), we found that maladaptive FSGS PECs expressed upregulated levels of integrin subunit beta 6 (*ITGB6*) and TGF-β-2 (*TGFB2*), pointing to activation of the TGF-β pathway, as was also seen in

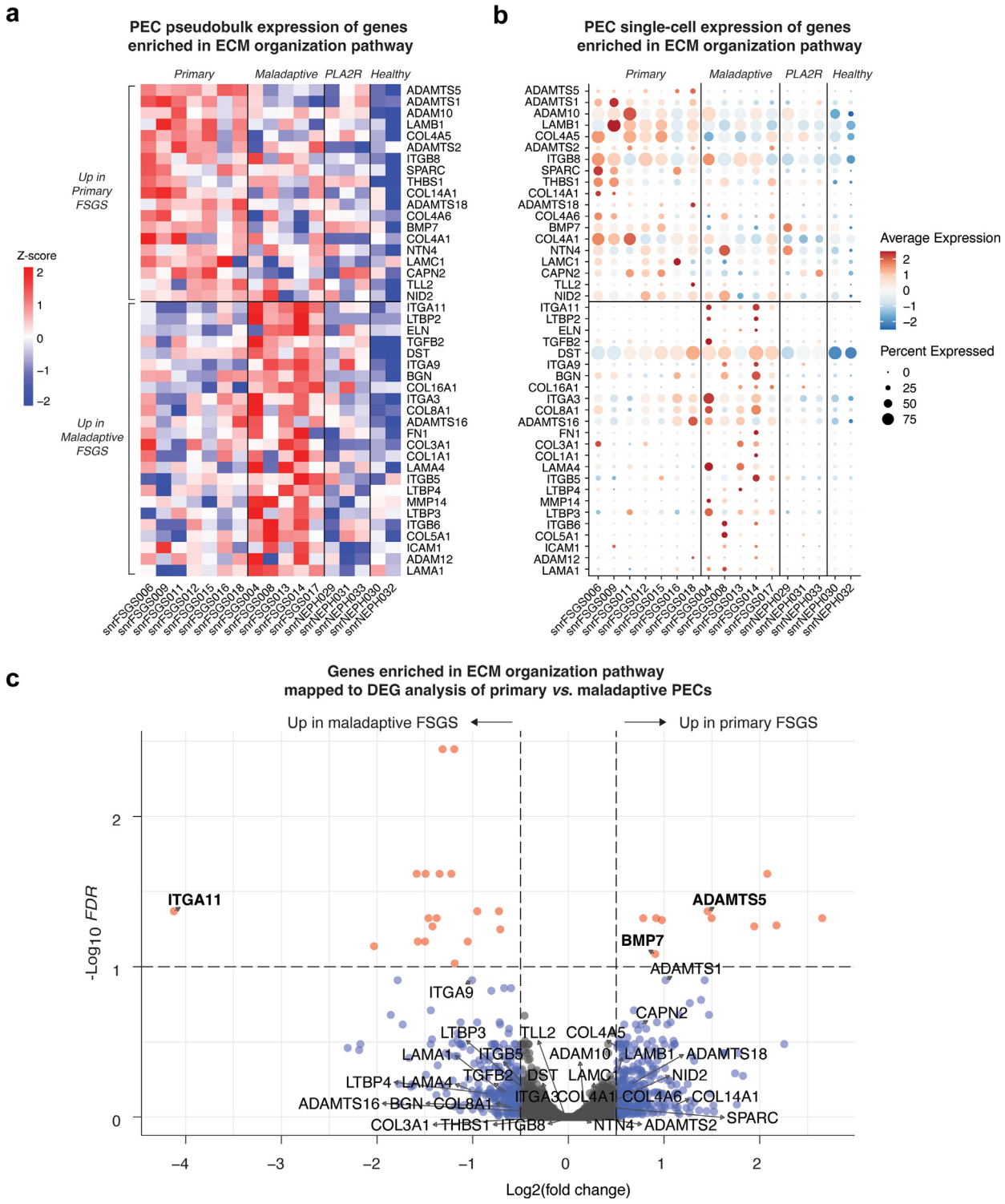


**Figure 4.** Differential expression of ECM signature in primary versus maladaptive FSGS PECs. (a) Heatmap showing pseudobulk gene expression in PECs of genes that were enriched in the "Extracellular Matrix Organization" Reactome-pathway (Figure 3d and e). These genes were significantly upregulated $>$ 0.25 $\log_2$FC (unadjusted *P*-value $<$ 0.05) in primary FSGS PECs versus other PECs and enriched in the ECM organization pathway upregulated in primary FSGS and/or these genes were significantly upregulated $>$ 0.25 $\log_2$FC (unadjusted *P*-value $<$ 0.05) in maladaptive FSGS PECs versus other PECs and enriched in the ECM organization pathway upregulated in maladaptive FSGS. Scale = z-score calculated per row. (b) Dot plot showing single-cell gene expression in PECs of the same ECM signature from panel a. The size of the dot reflects the fraction of cells (%) in which the gene is expressed, the color of the dot reflects average expression level. (c) Volcano plot depicting DEGs in primary FSGS PECs versus maladaptive FSGS PECs (red dots and gene names in bold indicate absolute $\log_2$FC $>$ 0.50 or $\log_2$FC $<$ −0.50, adjusted *P*-value (FDR) $<$ 0.10). Genes of the identified ECM-signature (panel a) are labeled on the Volcano plot. Upregulated genes are more specific for primary FSGS, downregulated genes are more specific for maladaptive FSGS. Genes in the middle of the plot are rather upregulated in both FSGS groups versus controls. DEG, differentially expressed gene; ECM, extracellular matrix; FSGS, focal segmental glomerulosclerosis; PEC, parietal epithelial cell.

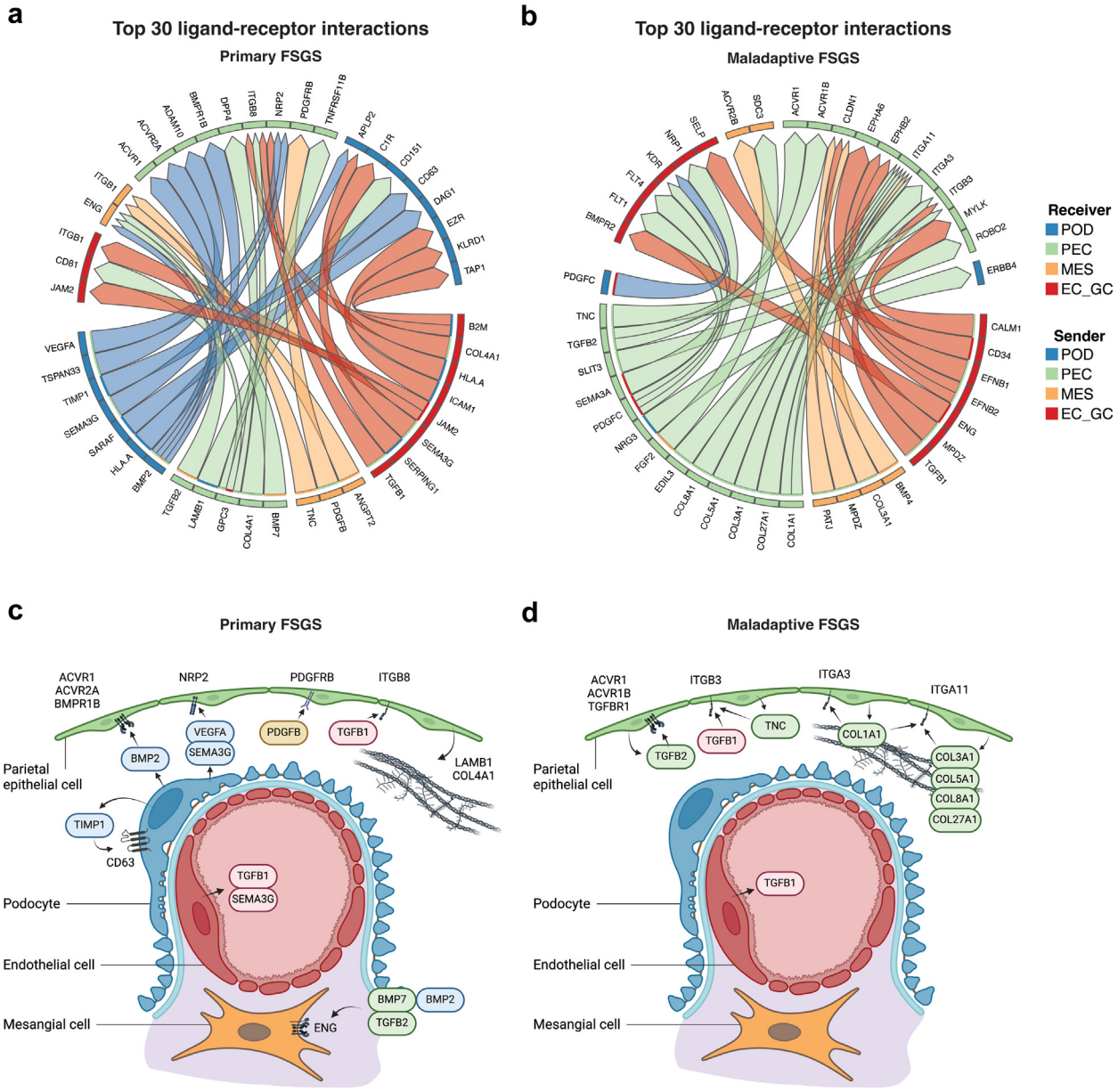


**Figure 5.** Differential glomerular cell-cell interactions in primary and maladaptive FSGS. Circos plot showing the 30 top-prioritized ligand-receptor interactions across all glomerular cells. (a) Top 30 ligand-receptor interactions in primary FSGS (ligand genes in sender cell types and receptor genes in receiver cell types are shown). (b) Top 30 ligand-receptor interactions in maladaptive FSGS (ligand genes in sender cell types and receptor genes in receiver cell types are shown). (c) Figure depicting glomerular cell-cell interactions in primary FSGS, based on differential cell-cell interactions and gene regulatory networks, derived from MultiNicheNet output. (d) Figure depicting glomerular cell-cell interactions in maladaptive FSGS, based on differential cell-cell interactions and gene regulatory networks, derived from MultiNicheNet output. EC_GC, glomerular capillary endothelial cell; FSGS, focal segmental glomerulosclerosis; MES, mesangial cell; PEC, parietal epithelial cell; POD, podocyte. Parts of panels (c) and (d) were made with BioRender.

primary FSGS PECs. However, a small subpopulation of maladaptive FSGS PECs exhibited a distinct (myo-) fibroblast-like phenotype, with heterogeneous upregulation of nontype IV collagens (*COL1A1*, *COL5A1*, *COL8A1*, *COL16A1*), glycoproteins (*FN1*, *ELN*, *LAMA1*, *LAMA4*), proteoglycans (*BGN*), and integrins (*ITGA11*) (Figure 4b). Of note, these PECs with stromal-like phenotypes were most abundant in 3 biopsy samples (4, 8, and 14). Taken together, maladaptive FSGS PECs also demonstrated a profibrotic response, but differed from primary FSGS by exhibiting a distinct (myo-)fibroblast-like subpopulation.

## Comparison of Matrisome Gene Expression in PECs and Mesangial Cells

A previous study reported transcriptional upregulation of biglycan (*BGN*) and collagen subunits (*COL1A1*, *COL1A2*, and *COL15A1*) in glomeruli of patients with FSGS; however, the cellular origin of this ECM signature remained unclear.[25] To clarify the contribution of

PECs and mesangial cells to this gene upregulation, we performed additional differential gene expression and GSEA (Supplementary Data S10 and S11) in mesangial cells (839 nuclei, *PDGFRB*+, *GATA3*+). Mesangial cells from primary FSGS upregulated pathways involved in integrin cell surface interactions, collagen formation and ECM organization (Supplementary Figure S19), whereas mesangial cells from maladaptive FSGS exhibited few DEGs and no upregulated pathways. Next, we directly compared the expression of collagens, proteoglycans, and glycoproteins (i.e., core matrisome genes[26]) in PECs versus mesangial cells (Supplementary Figure S20). Despite PECs being an epithelial rather than stromal cell type, overall core matrisome gene expression in FSGS PECs was not convincingly lower than mesangial cells. Some matrisome genes were specifically upregulated in maladaptive FSGS PECs, including collagens (*COL1A1*, *COL5A1*, *COL8A1*, and *COL16A1*) and glycoproteins (*ELN*, *LAMA1*, and *LAMA4*). Other genes were more abundantly expressed in primary FSGS mesangial cells, including collagen type III alpha 1 chain (*COL3A1*), biglycan (*BGN*), and fibronectin 1 (*FN1*). Taken together, in primary FSGS, mesangial cells may play a more prominent role in collagen formation and ECM deposition, whereas in maladaptive FSGS, a subpopulation of PECs acquire a stromal-like phenotype, which may contribute to nontype IV collagen deposition.

### Cell-cell Interactions Confirm Differential Profibrotic Signaling in Primary and Maladaptive FSGS

Finally, we used MultiNicheNet cell-cell interaction analysis to examine paracrine signaling in the glomerular microenvironment between diagnostic groups (Figure 5).[19] In primary FSGS, several interactions led to podocyte upregulation of the matrix metalloproteinase inhibitor *TIMP1* (Figure 5a, Supplementary Figure S21), which forms a complex with CD63 and β1-integrin, promoting cell adhesion, migration, proliferation, and survival.[27] *TIMP1* was also enriched in the ECM organization pathway in primary FSGS podocytes (Supplementary Figure S14), suggesting it could play a key role in primary FSGS pathophysiology. Other interactions in primary FSGS further confirmed a pivotal role for PECs in TGF-β-dependent and TGF-β-independent tissue fibrosis pathways (Figure 5a, Supplementary Figures S22 and S23). First, endothelial cells expressed TGF-β1 (*TGFB1*), which interacted with the integrin heterodimer αvβ8 (*ITGB8*) in PECs. Second, mesangial cells upregulated the TGF-β coreceptor endoglin (*ENG*), which may further promote TGB-β-signaling.[28] Third, mesangial cells upregulated *PDGFB*, which interacted with its receptor *PDGFRB* in PECs, leading to upregulation of *STAT1*, both of which were top DEGs in primary FSGS PECs (Figure 3a).

In maladaptive FSGS, podocytes no longer substantially participated in cellular crosstalk, whereas interactions between PECs predominated (Figure 5b). PECs interacted with each other via collagens and collagen binding integrins, again pointing to the presence of a profibrotic (myo-)fibroblast-like PEC subpopulation. Endothelial cells expressed TGF-β1 (*TGFB1*), PECs expressed TGF-β2 (*TGFB2*) and its receptor (*TGFBR1*), suggesting upregulated TGF-β signaling (Supplementary Figures S24 and S25). In summary, these cell-cell interaction analyses corroborated previous findings, with both FSGS subgroups showing activation of TGF-β signaling, while PDGFR-β signaling was specific for primary FSGS PECs, and a maladaptive FSGS PEC subpopulation specifically upregulated (myo-)fibroblast-like ECM genes.

## DISCUSSION

In this study, we used snRNA-seq to investigate the cellular heterogeneity, differential gene expression profile and crosstalk of glomerular cells in patients with primary FSGS, maladaptive FSGS and controls. A total of 120,751 nuclei passed stringent quality control filtering thresholds, and our analytic pipeline used pseudobulk differential gene expression methods to better account for intersample variability and reduce the risk of false discoveries.[17] Patients with FSGS were carefully subtyped,[2,6] and analyzed at single-cell resolution, yielding a high-quality and well-phenotyped dataset, that may also serve as a resource for future research.

We first investigated whether the presence of a circulating permeability factor in primary FSGS would translate into altered podocyte signal transduction. Primary FSGS podocytes upregulated genes involved in the innate immune system and antigen presentation, which were, to a lesser degree, also upregulated in maladaptive FSGS podocytes. A bulk RNA-seq study on glomeruli of patients with FSGS with high versus low risk *APOL1* genotype also found upregulation of the antigen presentation pathway in both groups, providing further evidence that immune pathways are upregulated in various podocytopathies.[29] Podocytes may indeed actively participate in both innate and adaptive immunity in various kidney diseases,[30] and have been shown to act as antigen-presenting cells by expressing major histocompatibility complex class I and II proteins, which in turn activate T cells.[31,32] Whether the upregulation of podocyte major histocompatibility complex class I genes in our study represents a primary initiating event that triggers a

subsequent immune response, or rather a secondary stress response to ongoing cell damage, remains unclear. Primary and, to a lesser extent, maladaptive FSGS podocytes upregulated the mTORC1 pathway. mTOR regulates podocytes size, and mTOR activation has been implicated in FSGS pathophysiology[33]; however, according to our data, this does not appear to be specific to one FSGS etiology.

We did, however, observe DEGs that were specifically upregulated in primary FSGS podocytes. TIMP metallopeptidase inhibitor 1 (*TIMP1)*, a soluble metalloproteinase inhibitor that is secreted into the extracellular environment,[27] was enriched in the podocyte ECM organization-pathway and emerged as a target gene in several ligand-receptor interactions in primary FSGS. TIMP1 inactivates several matrix metalloproteinases (MMPs, which degrade ECM), and TGF-β signaling leads to MMP/TIMP imbalance favoring fibrosis.[34,35] In addition, by forming a complex with its receptor CD63 and integrin subunit beta 1, TIMP1 can activate various signaling pathways in many different cell types, promoting cell adhesion, migration, proliferation, and survival.[27] A recent study on patients with primary podocytopathy (minimal change disease and FSGS) identified TIMP1 as a downstream effector and surrogate for intrarenal tumor necrosis factor–activation.[36] Patients with a high tumor necrosis factor score showed high *TIMP1*-expression in podocytes and fibroblasts, and high urinary protein levels of TIMP1 associated with poor outcomes.[36] In our dataset, 4 primary FSGS samples showed the highest podocyte *TIMP1*-expression, of which 2 patients experienced an adverse outcome (patient 6 developed disease relapse, patient 16 died 4 months after kidney biopsy). Primary FSGS podocytes upregulated *ECM1*, which is secreted to the ECM and, at least in liver fibrosis pathophysiology, has antifibrotic properties by protecting latent-TGF-β from activation.[37] It has been identified as a DEG in a microarray study on microdissected glomeruli of patients with FSGS,[38] and was upregulated in podocytes of an FSGS mouse model.[39] Nevertheless, podocyte upregulation of *ECM1* is likely not specific for FSGS, because it was also upregulated in glomeruli of patients with minimal change disease and MN.[40,41]

Next, we investigated the profibrotic response of PECs in primary and maladaptive FSGS. Primary FSGS PECs upregulated ADAMTS-enzymes, PDGFR-β signaling, and the TGF-β pathway, leading to upregulation of normal PEC basement membrane genes (collagen type IV and laminin subunit beta 1).[24] In mice,[8,42] rats,[9] and humans with FSGS,[9,10] PECs deposit Bowman's capsule matrix on the glomerular tuft in FSGS lesions, which, based on our data, is likely driven by TGF-β pathway and PDGFR-β signaling in PECs. A recent study also observed upregulation of PDGFR-β in PECs from both mice with FSGS lesions and patients with secondary FSGS.[42] Treatment of these mice with a PDGFB-neutralizing antibody reduced PEC proliferation, activation, and FSGS lesions, making PDGFR-b signaling an attractive candidate for antifibrotic treatment.[42] Interestingly, a recent study that applied a novel spatially resolved transcriptomics approach (whole-transcriptome GeoMx digital spatial profiling platform) on glomeruli of 2 patients with primary FSGS versus healthy controls further corroborated our findings: upregulated pathways in primary FSGS glomeruli included ECM organization, PDGF signaling, and collagen synthesis and degradation.[43] Moving forward, upregulation of PDGFR-β in PECs should be further investigated in human patients with different subtypes of FSGS, and the antifibrotic properties of PDGFB neutralizing antibodies should be further explored in other preclinical models of FSGS.

In maladaptive FSGS, PECs dominated the top cell-cell interactions. The TGF-β pathway, but not PDGFR-β signaling, was upregulated in maladaptive FSGS PECs, likely driving glomerulosclerosis. A small subpopulation of maladaptive FSGS PECs showed a profibrotic and (myo-)fibroblast-like phenotype with upregulation of fibril-forming collagens (*COL1A1*, *COL5A1*) and network-forming collagens (*COL8A1*). A recent study reanalyzed scRNA-seq data from 4 different glomerular disease mouse models,[44] and identified a PEC subcluster that increased collagen fibril organization in multiple types of glomerular injury.[45] Merchant *et al*. showed upregulation of *COL1A1* and *COL1A2* in glomeruli of patients with FSGS versus healthy controls, further suggesting that collagen type I expression is upregulated in FSGS. Moreover, *COL8A1* and *COL1A1* were among the top upregulated genes in a recent study that performed bulk RNA-seq on glomeruli of a subgroup of FSGS ($n = 50$) and minimal change disease ($n = 6$) patients with worse prognosis.[46] Notably, in our study, patients with high PEC *COL8A1* expression, either in primary or maladaptive FSGS, also showed an adverse outcome (patient 4 developed kidney failure, patients 6 and 12 showed disease relapse, patient 13 had a very high chronicity score on kidney biopsy, and patient 16 died). Maladaptive FSGS PECs also upregulated *ITGA11*, which preferentially binds to collagen type I. ITGA11 was previously found to be upregulated in human fibrotic kidneys, colocalizing with vascular smooth muscle cells and interstitial fibroblasts.[47] Therefore, *ITGA11* upregulation in PECs in our study further supports a potential profibrotic phenotype switch. Remarkably, the overall core matrisome gene expression in PECs was not convincingly lower than mesangial cells in FSGS, which

are the main glomerular ECM producing stromal cells.[48] However, the correlation between gene expression and ECM protein composition may be low,[25,49,50] and it is currently unclear whether the contribution of PECs in nontype IV collagen deposition is substantial. Furthermore, nuclei-seq data does not allow to spatially delineate whether these ECM proteins are deposited in the Bowman's space or at the mesangium.

Our study has some limitations. First, although we used strict diagnostic criteria to stratify patients across FSGS subtypes,[1,2,6] we cannot rule out that one or more 1 patients have been misclassified. Second, we did not include a separate genetic FSGS group. Third, as expected, patients with primary and those with maladaptive FSGS differed in the level of proteinuria and degree of chronicity on kidney biopsy, which could possibly confound some of our observations. Nevertheless, the difference in proteinuria is a defining feature that differentiates primary from maladaptive FSGS cases,[6] which was therefore difficult to account for. We only included patients with untreated primary FSGS, which were biopsied early in the disease course and frequently have a low degree of disease chronicity. Conversely, patients with maladaptive FSGS are often biopsied late in the disease course, and all candidate samples showed a high degree of chronicity, making it difficult to match chronicity levels to primary FSGS samples. Fourth, we did not perform additional protein expression validation studies. Nevertheless, our study for the first time provided a comprehensive kidney single-cell transcriptional landscape of patients with well-phenotyped primary and maladaptive FSGS.

In conclusion, patients with primary and those with maladaptive FSGS showed both overlapping and different potential disease mechanisms. In primary FSGS, podocytes exhibited a more pronounced but not specific injury pattern, with crosstalk to all other glomerular cells. This resulted in profibrotic TGF-β and PDGFR-β signaling and subsequent activation of PECs that upregulated and likely deposited Bowman's capsule ECM. In maladaptive FSGS, PEC-PEC interactions predominated and the TGF-β pathway and a distinct (myo-) fibroblast-like PEC subpopulation may contribute to glomerulosclerosis. Moving forward, spatial transcriptomics and proteomics studies may further validate the PECs' contribution to nontype IV collagen deposition in FSGS and further investigate whether such deposition is confined to the Bowman's space. The interplay between podocytes and PECs in FSGS certainly is a promising avenue for future research.

## DISCLOSURE

All the authors declared no competing interests.

## ACKNOWLEDGMENTS

We thank Dóra Bihary for her involvement and contribution to the preliminary bioinformatics data analysis. We would like to thank Robin Browaeys for assistance in the use of the MultiNicheNet R-package. We thank Dr. Laurens De Sadeleer for his input on the analysis of profibrotic PECs in maladaptive FSGS. We would also like to thank Professor Alejandro Sifrim for his input and suggestions regarding quality control metrics and cut-offs used in the analysis.

### Funding

DD is supported by a PhD Fellowship grant fundamental research from the Research Foundation Flanders (F.W.O.) (grant number 11L5622N). AHVC is supported by a postdoctoral grant from the University Hospitals Leuven (KOOR) and a Research Foundation Flanders (FWO) SBO project (S006722N). BKM is a senior clinical investigator of F.W.O. (1800820N) and received grant support from KU Leuven (3M190551 and C14/21/103).

## DATA AVAILABILITY STATEMENT

The snRNA-seq data supporting the findings of this study are available from European Genome-Phenome Archive (EGA) (dataset ID EGAS50000001070). Data requests will be reviewed by the UZLeuven-VIB data access committee and data can be released upon the signing of a Data Transfer Agreement that will include the necessary conditions to guarantee the protection of personal data (according to European GDPR law). R-scripts are openly available from GitHub repository (https://github.com/lambrechtslab/FSGS_Deleersnijder_et_al).

## AUTHOR CONTRIBUTIONS

AHVC confirms that she has had full access to the data in the study and final responsibility for the decision to submit for publication. DD, BS, DL, and AHVC conceived and designed the work that led to the submission. DD, TV, RS, TVB, BS and AHVC acquired the study data. DD, TV, RS, TVB, BKM, BS, DL, and AHVC played an important role in interpreting the results. DD drafted the manuscript, which was revised by TV, RS, TVB, BKM, BS, DL, and AHVC. DD, TV, RS, TVB, BKM, BS, DL, and AHVC approved the final version of the manuscript.

## SUPPLEMENTARY MATERIAL

Supplementary File (PDF and Excel)

**Supplementary Methods.**

**Supplementary References.**

**Figure S1.** Quality control parameters of the final dataset per sample.

**Figure S2.** Quality control parameters of the final dataset per diagnosis.

**Figure S3.** Quality control parameters of the final dataset per cluster.
**Figure S4.** Cell type abundance analysis in total kidney cell population.
**Figure S5.** Proportions of cell types per sample.
**Figure S6.** Quality control parameters of podocytes per sample.
**Figure S7.** Quality control parameters of podocytes per diagnosis.
**Figure S8.** GSEA in primary FSGS podocytes versus all other podocytes and versus only control podocytes.
**Figure S9:** Differential gene expression analysis in primary versus maladaptive FSGS podocytes.
**Figure S10.** Enriched genes in immune pathways in primary FSGS podocytes.
**Figure S11.** Enriched genes in mTORC1 signaling pathway in primary FSGS podocytes.
**Figure S12.** Podocyte gene expression of genes involved in genetic FSGS.
**Figure S13.** GSEA in maladaptive FSGS podocytes versus all other podocytes and versus only control podocytes.
**Figure S14.** Enriched genes in ECM-related pathways in all FSGS podocytes.
**Figure S15.** Quality control parameters of PECs per sample.
**Figure S16.** Quality control parameters of PECs per diagnosis.
**Figure S17.** GSEA in primary FSGS PECs versus all other PECs and versus only control PECs.
**Figure S18.** Differential gene expression analysis in primary versus maladaptive FSGS PECs.
**Figure S19.** Pathway analysis and enriched genes in primary FSGS mesangial cells.
**Figure S20.** Expression of core matrisome genes in PECs versus mesangial cells.
**Figure S21.** Differential cell-cell interactions and gene regulatory networks per diagnosis.
**Figure S22.** Top 50 glomerular cell interactions in primary FSGS.
**Figure S23.** Top 30 glomerular cell interactions with PEC as receiving cell type in primary FSGS.
**Figure S24.** Top 50 glomerular cell interactions in maladaptive FSGS.
**Figure S25.** Top 30 glomerular cell interactions with PEC as receiving cell type in maladaptive FSGS.
**Table S1.** Clinicopathologic characteristics of included patients with a diagnosis of primary or maladaptive FSGS.
**Table S2.** Clinicopathologic characteristics of included patients with a diagnosis of PLA2R+ MN.
**Table S3.** Clinicopathologic characteristics of included healthy controls.
STROBE Checklist.
**Data S1.** QC metrics per sample derived from Cell Ranger output.
**Data S2.** QC metrics per sample, diagnosis and cluster at main annotation level.
**Data S3.** Differentially expressed genes in the annotated cell clusters at main annotation level.
**Data S4.** Podocyte QC metrics, per sample and per diagnosis.
**Data S5.** EdgeR DGE analysis in podocytes comparing conditions.
**Data S6.** GSEA on EdgeR DEGs in podocytes comparing conditions.
**Data S7.** PEC QC metrics, per sample and per diagnosis.
**Data S8.** EdgeR DGE analysis in PECs comparing conditions.
**Data S9.** GSEA on EdgeR DEGs in PECs comparing conditions.
**Data S10.** EdgeR DGE analysis in mesangial cells comparing conditions.
**Data S11.** GSEA on EdgeR DEGs in mesangial cells comparing conditions.

## REFERENCES


1. De Vriese AS, Sethi S, Nath KA, Glassock RJ, Fervenza FC. Differentiating primary, genetic, and secondary FSGS in adults: A clinicopathologic approach. *J Am Soc Nephrol*. 2018;29:759–774. https://doi.org/10.1681/ASN.2017090958
2. De Vriese AS, Wetzels JF, Glassock RJ, Sethi S, Fervenza FC. Therapeutic trials in adult FSGS: lessons learned and the road forward. *Nat Rev Nephrol*. 2021;17:619–630. https://doi.org/10.1038/s41581-021-00427-1
3. Kopp JB, Anders HJ, Susztak K, et al. Podocytopathies. *Nat Rev Dis Primers*. 2020;6:68. https://doi.org/10.1038/s41572-020-0196-7
4. Shabaka A, Tato Ribera A, Fernandez-Juarez G. Focal segmental glomerulosclerosis: state-of-the-art and clinical perspective. *Nephron*. 2020;144:413–427. https://doi.org/10.1159/000508099
5. Miao J, Pinto EVF, Hogan MC, et al. Identification of genetic causes of focal segmental glomerulosclerosis increases with proper patient selection. *Mayo Clin Proc*. 2021;96:2342–2353. https://doi.org/10.1016/j.mayocp.2021.01.037
6. Rovin BH, Adler SG, Barratt J. KDIGO 2021 clinical practice guideline for the management of glomerular diseases. *Kidney Int*. 2021;100:S1–S276. https://doi.org/10.1016/j.kint.2021.05.021
7. Bronstein R, Pace J, Gowthaman Y, Salant DJ, Mallipattu SK. Podocyte-parietal epithelial cell interdependence in glomerular development and disease. *J Am Soc Nephrol*. 2023;34:737–750. https://doi.org/10.1681/ASN.0000000000000104
8. Smeets B, Kuppe C, Sicking EM, et al. Parietal epithelial cells participate in the formation of sclerotic lesions in focal segmental glomerulosclerosis. *J Am Soc Nephrol*. 2011;22:1262–1274. https://doi.org/10.1681/ASN.2010090970
9. Miesen L, Bandi P, Willemsen B, et al. Parietal epithelial cells maintain the epithelial cell continuum forming Bowman's space in focal segmental glomerulosclerosis. *Dis Model Mech*. 2022;15:dmm046342. https://doi.org/10.1242/dmm.046342

10. Smeets B, Stucker F, Wetzels J, et al. Detection of activated parietal epithelial cells on the glomerular tuft distinguishes early focal segmental glomerulosclerosis from minimal change disease. *Am J Pathol*. 2014;184:3239–3248. https://doi.org/10.1016/j.ajpath.2014.08.007
11. Deleersnijder D, Van Craenenbroeck AH, Sprangers B. Deconvolution of focal segmental glomerulosclerosis pathophysiology using transcriptomics techniques. *Glomerular Dis*. 2021;1:265–276. https://doi.org/10.1159/000518404
12. Slyper M, Porter CBM, Ashenberg O, et al. A single-cell and single-nucleus RNA-Seq toolbox for fresh and frozen human tumors. *Nat Med*. 2020;26:792–802. https://doi.org/10.1038/s41591-020-0844-1
13. Fleming SJ, Chaffin MD, Arduini A, et al. Unsupervised removal of systematic background noise from droplet-based single-cell experiments using CellBender. *Nat Methods*. 2023;20:1323–1335. https://doi.org/10.1038/s41592-023-01943-7
14. McGinnis CS, Murrow LM, Gartner ZJ. DoubletFinder: doublet detection in single-cell RNA sequencing data using artificial nearest neighbors. *Cell Syst*. 2019;8:329–337. https://doi.org/10.1016/j.cels.2019.03.003
15. Korsunsky I, Millard N, Fan J, et al. Fast, sensitive and accurate integration of single-cell data with Harmony. *Nat Methods*. 2019;16:1289–1296. https://doi.org/10.1038/s41592-019-0619-0
16. Robinson MD, McCarthy DJ, Smyth GK. edgeR: a Bioconductor package for differential expression analysis of digital gene expression data. *Bioinformatics*. 2010;26:139–140. https://doi.org/10.1093/bioinformatics/btp616
17. Squair JW, Gautier M, Kathe C, et al. Confronting false discoveries in single-cell differential expression. *Nat Commun*. 2021;12:5692. https://doi.org/10.1038/s41467-021-25960-2
18. Korotkevich G, Sukhov V, Budin N, et al. Fast gene set enrichment analysis. Preprint. Posted online February 01, 2021. bioRxiv 060012. https://doi.org/10.1101/060012.
19. Browaeys R, Gilis J, Sang-Aram C, et al. MultiNicheNet: a flexible framework for differential cell-cell communication analysis from multi-sample multi-condition single-cell transcriptomics data. Preprint. Posted online June 14, 2023. https://doi.org/10.1101/2023.06.13.544751. Posted online June 14, 2023. bioRxiv 2023.06.13.544751.
20. Sethi S, D'Agati VD, Nast CC, et al. A proposal for standardized grading of chronic changes in native kidney biopsy specimens. *Kidney Int*. 2017;91:787–789. https://doi.org/10.1016/j.kint.2017.01.002
21. Hengel FE, Dehde S, Lasse M, et al. Autoantibodies targeting nephrin in podocytopathies. *N Engl J Med*. 2024;391:422–433. https://doi.org/10.1056/NEJMoa2314471
22. Watts AJB, Keller KH, Lerner G, et al. Discovery of autoantibodies targeting nephrin in minimal change disease supports a novel autoimmune etiology. *J Am Soc Nephrol*. 2022;33:238–252. https://doi.org/10.1681/ASN.2021060794
23. Kelwick R, Desanlis I, Wheeler GN, Edwards DR. The ADAMTS (A disintegrin and metalloproteinase with thrombospondin motifs) family. *Genome Biol*. 2015;16:113. https://doi.org/10.1186/s13059-015-0676-3
24. Chan GC, Eng DG, Miner JH, et al. Differential expression of parietal epithelial cell and podocyte extracellular matrix proteins in focal segmental glomerulosclerosis and diabetic nephropathy. *Am J Physiol Ren Physiol*. 2019;317:F1680–F1694. https://doi.org/10.1152/ajprenal.00266.2019
25. Merchant ML, Barati MT, Caster DJ, et al. Proteomic analysis identifies distinct glomerular extracellular matrix in collapsing focal segmental glomerulosclerosis. *J Am Soc Nephrol*. 2020;31:1883–1904. https://doi.org/10.1681/ASN.2019070696
26. Naba A, Clauser KR, Hoersch S, Liu H, Carr SA, Hynes RO. The matrisome: in silico definition and in vivo characterization by proteomics of normal and tumor extracellular matrices. *Mol Cell Proteomics*. 2012;11:M111.014647. https://doi.org/10.1074/mcp.M111.014647
27. Justo BL, Jasiulionis MG. Characteristics of TIMP1, CD63, and β1-Integrin and the functional impact of their interaction in cancer. *Int J Mol Sci*. 2021;22:9319. https://doi.org/10.3390/ijms22179319
28. Derynck R, Budi EH. Specificity, versatility, and control of TGF-beta family signaling. *Sci Signal*. 2019;12:eaav5183. https://doi.org/10.1126/scisignal.aav5183
29. McNulty MT, Fermin D, Eichinger F, et al. A glomerular transcriptomic landscape of apolipoprotein L1 in Black patients with focal segmental glomerulosclerosis. *Kidney Int*. 2022;102:136–148. https://doi.org/10.1016/j.kint.2021.10.041
30. Jiang H, Shen Z, Zhuang J, et al. Understanding the podocyte immune responses in proteinuric kidney diseases: from pathogenesis to therapy. *Front Immunol*. 2023;14:1335936. https://doi.org/10.3389/fimmu.2023.1335936
31. Goldwich A, Burkard M, Olke M, et al. Podocytes are nonhematopoietic professional antigen-presenting cells. *J Am Soc Nephrol*. 2013;24:906–916. https://doi.org/10.1681/asn.2012020133
32. Li S, Liu Y, He Y, et al. Podocytes present antigen to activate specific T cell immune responses in inflammatory renal disease. *J Pathol*. 2020;252:165–177. https://doi.org/10.1002/path.5508
33. Zschiedrich S, Bork T, Liang W, et al. Targeting mTOR signaling can prevent the progression of FSGS. *J Am Soc Nephrol*. 2017;28:2144–2157. https://doi.org/10.1681/ASN.2016050519
34. Czirok S, Fang L, Radovits T, et al. Cinaciguat ameliorates glomerular damage by reducing ERK1/2 activity and TGF-ß expression in type-1 diabetic rats. *Sci Rep*. 2017;7:11218. https://doi.org/10.1038/s41598-017-10125-3
35. Kokeny G, Nemeth A, Kopp JB, et al. Susceptibility to kidney fibrosis in mice is associated with early growth response-2 protein and tissue inhibitor of metalloproteinase-1 expression. *Kidney Int*. 2022;102:337–354. https://doi.org/10.1016/j.kint.2022.03.029
36. Mariani LH, Eddy S, AlAkwaa FM, et al. Precision nephrology identified tumor necrosis factor activation variability in minimal change disease and focal segmental glomerulosclerosis. *Kidney Int*. 2023;103:565–579. https://doi.org/10.1016/j.kint.2022.10.023
37. Fan W, Liu T, Chen W, et al. ECM1 Prevents Activation of transforming growth factor beta, Hepatic Stellate Cells, and fibrogenesis in Mice. *Gastroenterology*. 2019;157:1352–1367. https://doi.org/10.1053/j.gastro.2019.07.036
38. Gholaminejad A, Ghaeidamini M, Simal-Gandara J, Roointan A. An Integrative in silico Study to DISCover Key Drivers in Pathogenicity of Focal and Segmental glomerulosclerosis. *Kidney Blood Press Res*. 2022;47:410–422. https://doi.org/10.1159/000524133

39. Potter AS, Drake K, Brunskill EW, Potter SS. A bigenic mouse model of FSGS reveals perturbed pathways in podocytes, mesangial cells and endothelial cells. *PLoS One*. 2019;14: e0216261. https://doi.org/10.1371/journal.pone.0216261
40. Li D, Liu L, Murea M, Freedman BI, Ma L. Bioinformatics analysis reveals a shared pathway for common forms of adult nephrotic syndrome. *Kidney360*. 2023;4:e515–e524. https://doi.org/10.34067/KID.0000000000000074
41. Feng X, Chen Q, Zhong J, et al. Molecular characteristics of circulating B cells and kidney cells at the single-cell level in special types of primary membranous nephropathy. *Clin Kidney J*. 2023;16:2639–2651. https://doi.org/10.1093/ckj/sfad215
42. Jia T, Xu T, Smeets B, et al. The role of platelet-derived growth factor in focal segmental glomerulosclerosis. *J Am Soc Nephrol*. 2023;34:241–257. https://doi.org/10.1681/ASN.2022040491
43. Clair G, Soloyan H, Cravedi P, et al. The spatially resolved transcriptome signatures of glomeruli in chronic kidney disease. *JCI Insight*. 2024;9:e165515. https://doi.org/10.1172/jci.insight.165515
44. Chung JJ, Goldstein L, Chen YJ, et al. Single-cell transcriptome profiling of the kidney glomerulus identifies key cell types and reactions to injury. *J Am Soc Nephrol*. 2020;31: 2341–2354. https://doi.org/10.1681/ASN.2020020220
45. Liu WB, Huang GR, Liu BL, et al. Single cell landscape of parietal epithelial cells in healthy and diseased states. *Kidney Int*. 2023;104:108–123. https://doi.org/10.1016/j.kint.2023.03.036
46. Hodgin JB, Mariani LH, Zee J, et al. Quantification of glomerular structural lesions: associations with clinical outcomes and transcriptomic profiles in nephrotic syndrome. *Am J Kidney Dis*. 2022;79:807–819. https://doi.org/10.1053/j.ajkd.2021.10.004
47. Bansal R, Nakagawa S, Yazdani S, et al. Integrin alpha 11 in the regulation of the myofibroblast phenotype: implications for fibrotic diseases. *Exp Mol Med*. 2017;49:e396. https://doi.org/10.1038/emm.2017.213
48. Avraham S, Korin B, Chung JJ, Oxburgh L, Shaw AS. The mesangial cell - the glomerular stromal cell. *Nat Rev Nephrol*. 2021;17:855–864. https://doi.org/10.1038/s41581-021-00474-8
49. Liu Y, Beyer A, Aebersold R. On the dependency of cellular protein levels on mRNA abundance. *Cell*. 2016;165:535–550. https://doi.org/10.1016/j.cell.2016.03.014
50. Lausecker F, Lennon R, Randles MJ. The kidney matrisome in health, aging, and disease. *Kidney Int*. 2022;102:1000–1012. https://doi.org/10.1016/j.kint.2022.06.029